RESEARCH ARTICLE OPEN ACCESS

Study of electric discharge machining parameters for Al 6063/Al_2O_3 metal matrix composites using Taguchi Approach

Mina A. Hanna *,Sameh S. Habib**, Samah S. Mohamed**, Sayed Abdel-Wanis**
*(Faculty of Engineering, modern academy, Cairo, Egypt)
** (Shoubra Faculty of Engineering, Benha University, Cairo, Egypt)

Abstract:

In the present investigation, the effect of Electric discharge machining process parameters, namely peak current (I_p), duty cycle (D_t) and spark duration time (T_{on}) on the predominant machining evaluation criteria such as material erosion rate (MER), electrode wear rate (EWR), gap sides (2GS) and surface roughness (SR) were studied. Stir casting technique was used to prepare aluminum based metal matrix composite reinforced with Nano - alumina Al_2O_3 of average size 30 nm. The matrix Al (6063), Al - 0.5%Al_2O_3, Al-1%Al_2O_3 and Al-1.5%Al_2O_3 are selected as work-piece material. Graphite was used as an electrode material. L16 (4^4) orthogonal array based on Taguchi approach was used to design the machining experiments. The distribution of Al_2O_3 particles in as casted work was measured using optical microscope. Signal-to-noise ratio S/N and ANOVA analysis of variance are used to study the effect of process parameters on the surface roughness (SR),material erosion rate (MER), electrode wear rate (EWR) and gap side(2GS). It can be concluded that the current is the most significant impact on material erosion rate, electrode wear rate, surface roughness and gap side for graphite electrode.

Keywords **—Electrical discharge machining (EDM), Al6063/Al_2O_3, Taguchi approach, ANOVA, material erosion rate, electrode wear rate, surface roughness, gap side and stir casting technique.**

I. INTRODUCTION

Nowadays the rapid development in the technology led to increase the need of nano-composite material in manufacturing industries [1]. Nano-composite material occupies a wider domain in numerous commercial, architectural and industrial applications such as transport and in aviation, automotive and military industries. Nano-composites vary from traditional composite materials due to it can extremely enhance mechanical, electrical and chemical properties. For mechanical properties their hardness, strength and wear corrosion resistance were increased relative to low density.

The series of Al-Mg- Si alloys 6XXX have been extensively used as moderate strength structural alloys which have the advantages of good weldability, corrosion resistance, and eliminate the corrosion stress of cracking. However, very little researches have been applied on the usage of Al alloy (6063) as metal matrix [2].

The selection of Alumina as the reinforcement particles in Aluminum matrix is primarily intended to use the composite of high hardness, while its hardness provide it the advantage to be used as a reinforcement agent in MMC[1].

The use of non-traditional machining techniques in the machining of aluminum metal matrix composites (Al-MMC) has aroused considerable interest as it is difficult for the manufacturing a complex contours in these very hard materials at a high level of precision and surface finish [3]. Among the many non-traditional processing strategies, electrical discharge (ED) machining has proved itself to be one of the effective machining process in in a numerous industries including micro- electronics, injection mould and dies, intricate groves, surgical components stamp and biomedical industries [4]. Electrical Discharge (ED) Machining is thermo- electric process in which electrically conductive materials removed by a series of rapidly repeated discharging sparks when the applied volt exceed the breakdown voltage between electrodes and specimen in the presence of

dielectric fluid [5]. A channel of strong electromagnetic flux called plasma channel is formed. The strongest electrical field occurs at the closest point between the electrode and specimen [6]. The density of this electric field energy 1011 - 1014 W/m^2[7]. Resulting in a single spark is discharged in the channel [8]. Spark temperature is 6000-12000°C relying on the cutting conditions [7]. The electrode and specimen material melt and vaporize within this plasma channel.

In this study, experiment was planned using orthogonal array L16 (4^4) by the Taguchi approach and electric discharge machining was applied on Al (6063), Al - 0.5%Al_2O_3, Al-1%Al_2O_3 and Al-1.5%Al_2O_3 as work-piece materials and by using graphite electrode.

II. EXPERIMENTAL WORK

The experiments were performed on a NC die sinking EDM (EMCO of ENGEMAQ EDM 200 NC) as shown in Fig. 1. The specification of EDM machine is tabulated in Table 1. A commercial grade odorless kerosene type (Flash point> 61°C and Specific Gravity at 15°C= 0.797) used as flushing fluid. Short cylindrical bars of graphite materials of 20 mm in diameter and 100mm in length were used as electrode. In this work, the electrodes were drilled by internal hole of 6 mm diameter for injection flushing as shown in Fig. 2. The chemical composition and physical properties are provided in Tables 2 and 3 respectively. Different settings of four controllable factors such as discharge current, spark duration time, material and duty cycle were used in the experiments. The polarity is positive when using graphite as tool electrodes. The working conditions of EDM are as listed in Table 4. The workpieces Al 6063, Al - 0.5%Al_2O_3, Al-1%Al_2O_3 and Al- 1.5% Al_2O_3 metal matrix composite. The chemical composition and properties of matrix material were provided in Table 5. Stir casting method was used to prepare the workpieces. The work piece is weighed before and after each experiment using a digital balance (SCATEC SBA41) with a resolution of 0.001 g to determine the value of material removal rate and electrode wear rate. Material erosion rate is computed as following equation (1),

$$MER = \frac{w_{wi} - w_{wf}}{t} \ldots\ldots\ldots(1)$$

Where MER is the material erosion rate (mm^3/min),w_{wi} is the initial average weight of the workpiece (g), $w_{wf}$is the final average weight of the workpiece (g), t is the machining time (min). Electrode wear rate is computed as following equation (2),

$$EWR = \frac{w_{ei} - w_{ef}}{t} \ldots\ldots\ldots(2)$$

Where EWR is the electrode wear rate (mm^3/min), $w_{ei}$is the initial average weight of the electrode (g), $w_{ef}$is the final average weight of the electrode (g), t is the machining time (min).

The gap side (2GS) value is determined based upon the results from Equation 3. The scanned holes diameter measured using 'JMicroVision 1.2.7' software.

$$2GS = D_H - D_E \ldots\ldots\ldots(3)$$

Where D_H is the hole diameter in mm and D_E is the electrode diameter in mm.

The surface roughness (SF) value Ra (mm) was measured using a 'Time TR200' portable surface measuring unit with a diamond stylus of a radius 5 µm. The cutoff length for each measurement was taken as 0.8 mm.

Table 1 EDM machine specification.

Parameters	Input current Ip (A)	Spark on time T_{on} (µs)	Duty cycle D_t(%)	Gap voltage V (v)	Flushing pressure P (Kg/cm2)
Range	0-80	1-999	1-99%	0-300	0-1.5

Table 2 chemical composition of graphite electrode

O	Na	Mg	Al	Si	S	Cl	K	Ca	Fe	Zn	C
0.152	0.035	0.001	0.002	0.002	0.038	0.023	0.005	0.005	0.008	0.002	99.7

Table 3 physical properties of graphite electrode.

Porosity (%)	Density g/cm3	Specific Heat J/(kg * K)	Melting Temperature °C	Thermal conductivity w/mk
0.7-53	1.3-1.95	710-830	3500	25-470

Table 4 EDM working condition

Condition name	Electrode type
	Graphite
Discharging current (I)	2, 4, 5 and 6
Spark duration time (Ton)	50, 100,150 and 200
Duty cycle (Dt)	83, 85, 87 and 91
Material (v%)	Al 6063, Al - 0.5%Al_2O_3, Al-1%Al_2O_3 and Al- 1.5% Al_2O_3
Flushing fluid	Odorless kerosene
Polarity	Positive
Pressure of Dielectric	1.5 kg/cm^2
Arc Gap	Constant
Machining depth	1 mm

Table 5 chemical composition of Al 6063

Sample specification of AL 6063	Magnesium (Mg)	Silicon (Si)	Iron (Fe)	Manganese (Mn)	Zinc (Zn)	Titanium (Ti)	Chromium (Cr)	Copper (Cu)	Aluminum (Al)
	0.415	0.408	0.21	0.016	0	0.012	0.02	0.0002	98.9

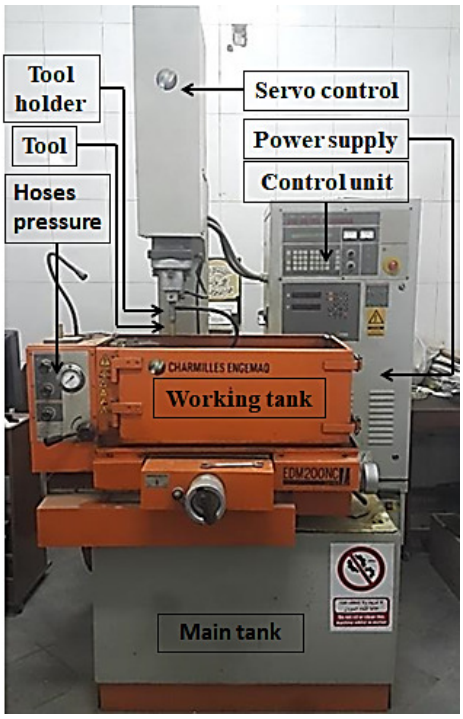

Fig. 1 EDM machine.

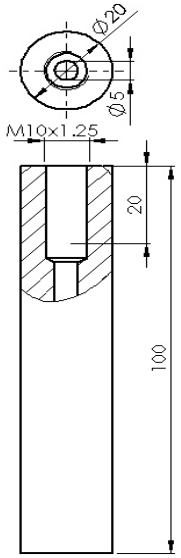

Fig. 2 graphite electrode

III. STIR CASTING SETUP

The selected work piece material were Aluminum 6063 and Al-Al_2O_3 metal matrix composite where Aluminum 6063 base metal and 0.5%, 1%, 1.5% Al_2O_3 as reinforcement particles. Firstly, the base metal Al 6063 was charged into graphite crucible and then heated inan electric resistance furnace as presented in Fig. 3 to a temperature of 750^{o}c from 3 to 4 hours to melt the base metal completely, generally it is melted above the liquidus temperature by 50^{o}c [9], [10], [11], [2],[11]and [12]. Meanwhile, the alumina particles (Al_2O_3 of 0.5%, 1%, 1.5%v) were preheated in electric resistance furnace to a temperature of 250^{o}c for 15 min. In order to get rid of the gas layer surrounding the particles and providing a better opportunity for slurry come in a contact with the surface of the

reinforcement particle [13], [14], [15], [11], [2]and [16]. Then, The liquid metal was left to cool in a furnace to a semi-solid phase at a temperature approximately 600°c[2],[17],[12] and [15]. At this temperature, the preheated Al_2O_3 particles were added gradually at constant rate, taking about 3 min in order to get a good incorporation. , while the mechanical stirring of the slurry had performed manually and with the help of automatic stirring of steel stirrer fixed in radial drilling machine at speed 200 rpm before adding the particles. The stirring was continued for 1 min after all the particles were introduced[18], [19], [12], [20], [21]and[11]. After the incorporation of the particles into the slurry, in order to perform a homogeneous and uniform distribution of particles, the composite slurry was superheated to 720°c[2],[17], [15],[12] and [22]. The second stirring of molten metal was performed under the surface of molten metal at 300 rpm for 5min[12],[2]. Finally, the molten composite was poured into preheated rectangular cast iron mould 565°c as shown in Fig. 4. Due to vigorously stirring of the slurry gases were entrapped, which is very difficult to be removed as a result of the high viscosity of slurry[9], [23],[24]and [25]. In addition to the air bubbles were sucked during the second stirring of the molten metal, so all sides of the preheated mould was covered by the salt Nacl. Nacl absorbs the oxygen, as it has a higher affinity to interact with oxygen than aluminum.

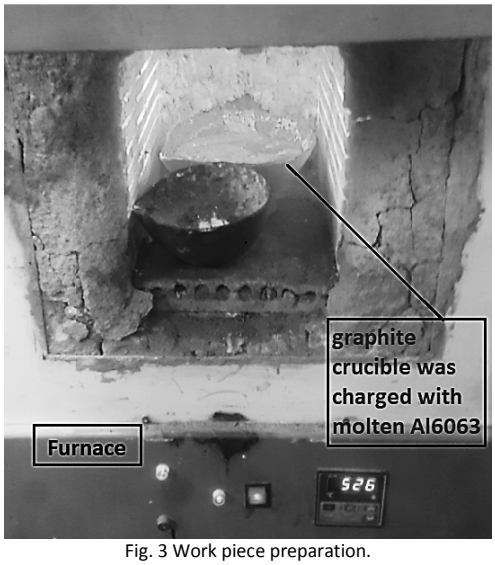

Fig. 3 Work piece preparation.

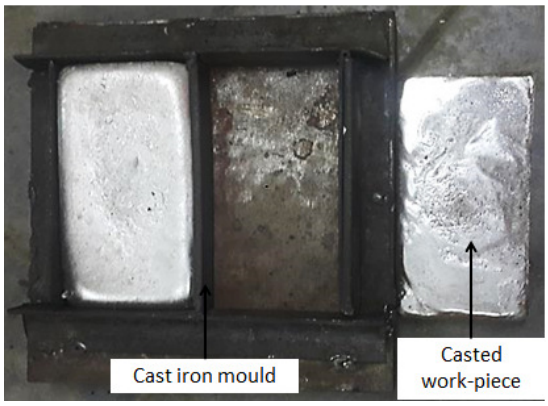

Fig. 4 Casted work piece.

IV. DESIGN OF EXPERIMENTS (DOE)

This experimental investigation is established based on selecting four controllable parameters from a several EDM factors, this parameter is currently (I), spark duration time (T_{on}), duty cycle (D_t) and material volume fraction (v%). Taking in consideration four levels for each controllable parameter as it is presented in Tables 6.

Taguchi was conducted to specify an optimal number of experiments for designing the experiment as well as to optimize the machining parameters for maximizing material erosion rate (MER), minimizing surface roughness (SR), gap size (2GS) and electrode wear rate (EWR) in EDM process

Taguchi technique is a statistical approach providing an effective and briefly number of experiments by transforming the experimental data into input factors and levels. Furthermore, orthogonal array estimates the impacts of input parameters on the response mean and deviation.The control factors are hired to select the best stability conditions in the design of machining process by

EDM, whilst the noise factors used to indicate all factors that give a variation.

This investigation is applied to study the effect of four control factors, as listed in Table 6. And then the experiment outputs are turned into (S/N) signal-to-noise ratio. The selecting of (S/N) ratio relies on the type of criteria which give the best machining performance. The higher value criteria give the best machining performance in the case of MER, and is termed 'higher is better, HB'. On the otherwise, the lower value criteria give the best machining performance in the case of electrode wear rate, surface roughness and gap side, and are termed 'lower is better, LB'. Therefore, HB for the MER, LB for the EWR, SR, and 2GS. The loss function (L) for the criteria of HB and LB is shown in equation 4, 5, 6 and 7:

$$L_{HB} = \frac{1}{n}\sum_{i=1}^{n}\frac{1}{y^2{}_{MER}} \text{.....(4)}$$

$$L_{LB} = \frac{1}{n}\sum_{i=1}^{n} y^2{}_{EWR} \text{.....(5)}$$

$$L_{LB} = \frac{1}{n}\sum_{i=1}^{n} y^2{}_{SR} \text{.....(6)}$$

$$L_{LB} = \frac{1}{n}\sum_{i=1}^{n} y^2{}_{2GS} \text{.....(7)}$$

Where the terms $y^2{}_{MER}$, $y^2{}_{EWR}$, $y^2{}_{SR}$ and $y^2{}_{2GS}$signed to the response for metal erosion rate, electrode wear rate, surface roughness and gap side, respectively, and n denotes the number of experiments run.

The S/N ratio response parameter can be calculated as a logarithmic transformation of the loss function as shown by equation from 8 to11.

$$\frac{S}{N} ratio for MER = -10\ \log_{10}(L_{HB}) \text{.....(8)}$$

$$\frac{S}{N} ratio for EWR = -10\ \log_{10}(L_{LB}) \text{.....(9)}$$

$$\frac{S}{N} ratio for SR = -10\ \log_{10}(L_{LB}) \text{.....(10)}$$

$$\frac{S}{N} ratio for\ 2GS = -10\ \log_{10}(L_{LB}) \text{.....(11)}$$

In the present research study, an L16 (4^4) orthogonal array was chosen with 16 rows corresponding the number of experiment and it has been repeated three times. By using Taguchi's orthogonal array, the overall number of 16 experiments was performed by several combinations of input factors. MINITAB 17software was conducted to analysis the experimental data, which is mainly used for the applications of experimental design (DOE).

V. Results and Discussion

Figure 5 presents the shape of work-piece after ED machining. The observations of machining experiments are investigated by using the S/N and ANOVA analyses. Based on the analysis of these observations, optimal machining parameters which maximize the material erosion rate and minimize the surface roughness, electrode wear rate and gap size are obtained. A set of 16 experiments is conducted in electric discharge machine for the graphite electrode. After conducting each experiment the material erosion ratio and electrode wear rate were calculated while surface roughness and gap size were measured. Signal-to-noise (S/N) ratios were a determined for each experiment as shown in Table 8. The responses of MER, EWR, SR and 2GS are analyzed using Taguchi and ANOVA analysis, which present the contribution of each input factor on MRR, EWR, SR and 2GS

Table 6 Factors and their levels.

process parameter	coding	level			
		1	2	3	4
Current (I)	A	2	4	5	6
Spark duration time (Ton)	B	50	100	150	200
Duty cycle (Dt)	C	83	85	87	91
Material (v%)	D	0	0.5	1	1.5

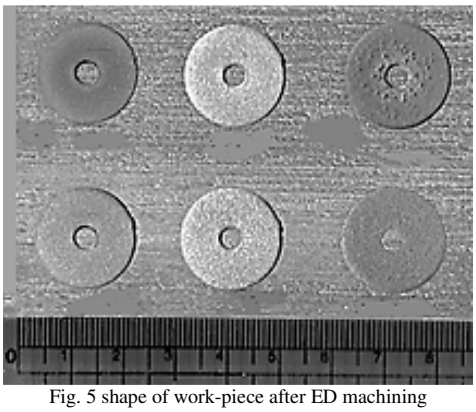

Fig. 5 shape of work-piece after ED machining

Table 7 Experimental design using L16 orthogonal array

Exp no.	A	B	C	D	MER	S/N	EWR	S/N	2GS	S/N	SR	S/N
1	2	50	83	0	0.01705	-35.36723	0.001214343	58.31317	20.3395	-26.166805	3.067	-9.7342755
2	4	100	85	0	0.07712	-22.25622	0.002183688	53.21619	20.4035	-26.194093	4.4	-12.869054
3	5	150	87	0	0.14919	-16.52517	0.003307182	49.61084	20.531	-26.248202	7.31	-17.278348
4	6	200	91	0	0.22516	-12.95011	0.000798446	61.95509	20.573	-26.265953	9.255	-19.327528
5	2	100	87	0.5	0.01237	-38.15522	0.003930365	48.11134	20.361	-26.175982	4.417	-12.902548
6	4	50	91	0.5	0.1012	-19.89628	0.048801852	26.23127	20.446	-26.212167	5.159	-14.251311
7	5	200	83	0.5	0.14457	-16.79815	0.015589297	36.14347	20.467	-26.221084	7.162	-17.100686
8	6	150	85	0.5	0.23203	-12.68912	0.015252312	36.33329	20.4885	-26.230203	7.651	-17.674364
9	2	150	91	1	0.00883	-41.07726	0.001559601	56.13973	20.3185	-26.157833	4.533	-13.127714
10	4	200	87	1	0.04782	-26.40709	0.007843409	42.1099	20.425	-26.203241	5.202	-14.323407
11	5	50	85	1	0.17742	-15.01982	0.081448433	21.78235	20.4675	-26.221296	6.406	-16.131739
12	6	100	83	1	0.19448	-14.22254	0.048217945	26.33583	20.4885	-26.230203	10.13	-20.112189
13	2	200	85	1.5	0.00725	-42.78773	0.001234826	58.16789	20.4475	-26.212804	4.847	-13.70946
14	4	150	83	1.5	0.06171	-24.19275	0.00663559	43.56241	20.4905	-26.231051	5.517	-14.83406
15	5	100	91	1.5	0.17685	-15.04788	0.026825633	31.429	20.553	-26.257504	6.343	-16.045894
16	6	50	87	1.5	0.25776	-11.7756	0.115121772	18.77685	20.5755	-26.267008	7.86	-17.908451

***A.* Effect of process parameters on MER**

In Fig. 6, main effect plots for S/N signal to noise ratio of material erosion rate (MER) for graphite electrodes are plotted as it clarified.If the line for a process parameter is almost horizontally, then the parameter has no statistically significant effect and therefore this parameter has no practically significant. Otherwise, if the line for a process parameter is almost vertically, then the parameter has the most significant effect.From Fig. 6, It is very clear from the main effect plots that current (A) is the most significant process parameter, while pulse duration time(B), material v% (D) and duty cycle (C) possess the following effect respectively.According to the higher-the-better quality criteria for MER of copper electrode, based on the maximum point on the graph, the optimum condition for each factor indicated is A4 (6 A), B1 (50 μs), C4 (91%), D1 (0 v%).

The S/N ratio is an indicator of the larger variance of the output characteristics around the desired value. The higher value of MER represents better criteria of machining performance, so the largest value of MER assigned by the largest value of S/N ratio. The mean S/N ratio for each level of the cutting parameters is summarized and called the mean S/N response table for material erosion rate Table 9. The impact of process parameters can be ranked as follows (current, pulse duration time, material and duty cycle).

ANOVA is a statistical technique that can be used to analysis the experimental data. The method is very useful for revealing the contribution level of factor(s) on a particular response. Table 10 presents

the ANOVA results for material removal rate. The ANOVA table presents the contribution percentage and the statistical significance of each parameter. Therefore, comparing between the P-value and generally used α-level = 0.05, it is found that if the P-value for each parameter is less than or equal to α, it can be indicated that the impact of this parameter is significant; otherwise it is not significant impact. The most effective parameter on MER is current (A) with contribution percentage (95.98%) followed by spark duration time (B) 2.06%, duty cycle (C) 1.10% and material (D) 0.071% is the least effective parameter.

The mathematical model is developed to relate the response parameters (EWR, MER, SR and 2GS) with their machining parameters (current, spark duration time, material and duty cycle) to facilitate the optimization process for machining the Al (6063), Al - 0.5%Al_2O_3, Al-1%Al_2O_3 and Al-1.5%Al_2O_3. The second degree polynomial regression analysis by Matlab R 2013b software was used to provide the following mathematical models.

$$\begin{aligned}\mathbf{MER} = &-8.823289096 + 1.074850309\text{x}10^{-1}\text{A} + 7.619891626\text{x}10^{-4}\text{B} + 2.023261294\text{x}10^{-1}\text{C} \\ &- 5.914707197\text{x}10^{-1}\text{D} + 2.830996254\text{x}10^{-4}\text{AB} - 1.680847627\text{x}10^{-3}\text{AC} \\ &- 3.67499086\text{x}10^{-2}\text{AD} - 3.592760606\text{x}10^{-5}\text{BC} - 4.516657952\text{x}10^{-4}\text{BD} \\ &+ 8.933949468\text{x}10^{-3}\text{CD} \\ &+ 1.007470324\text{x}10^{-2}\text{A}^2 + 3.795618459\text{x}10^{-6}\text{B}^2 - 1.140337726\text{x}10^{-3}\text{C}^2 \\ &+ 3.974228418\text{x}10^{-2}\text{D}^2 \ldots\ldots\ldots\ldots (12)\end{aligned}$$

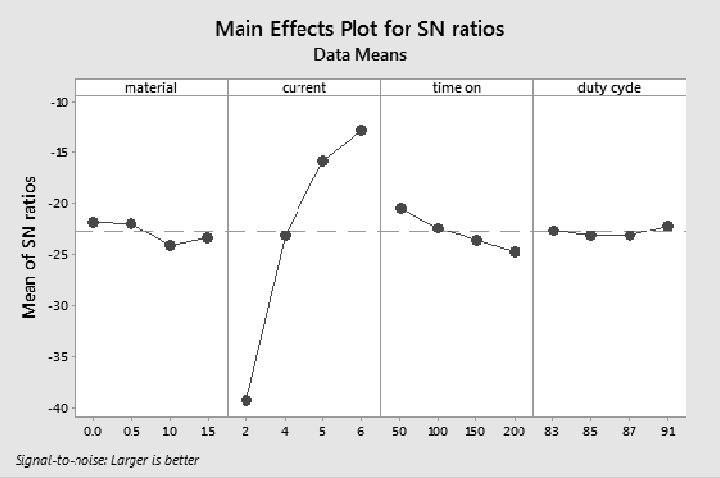

Fig. 6Main effects plot for S/N ratios of each factor on MER.

Table 8S/N ratio response table for MER

Level	Material	Current	Time on	Duty cycle
1	-21.77	-39.35	-20.51	-22.65
2	-21.88	-23.19	-22.42	-23.19
3	-24.18	-15.85	-23.62	-23.22
4	-23.45	-12.91	-24.74	-22.24
Delta	2.41	26.44	4.22	0.97
Rank	3	1	2	4

Table 9 ANOVA results for MER.

Sequence of variation	Degrees of freedom (DF)	Sum of squares (SS)	Mean square MS = SS/DF	Contribution	P-Value

material	3	0.000806	0.000269	0.71%	0.117
current	3	0.109536	0.036512	95.98%	0
time on	3	0.002348	0.000783	2.06%	0.029
duty cycle	3	0.00126	0.00042	1.10%	0.067
Error	3	0.000171	0.000057	0.15%	
Total	15				

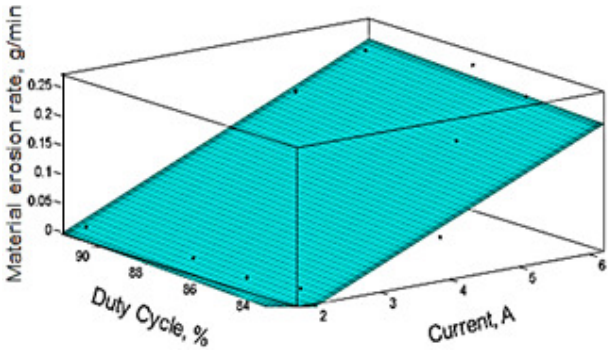

Fig. 7:Surface plot of material erosion rate versus current and duty cycle.

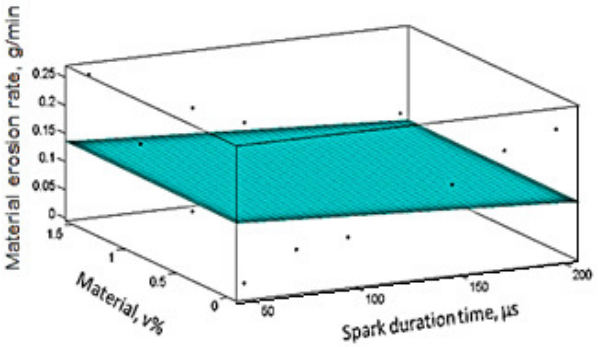

Fig. 8:Surface plot of material erosion rate versus material and spark duration time.

The surface curve fitting plot of a first polynomial degree present the relative effect of current and duty cycle on MER as it is shown in Figure. 7. It is clarified that the MER Increases significantly with increasing the current and this increase becomes more with increasing the duty cycle. The studies were demonstrated that The MER Material erosion rate increases by increasing the current density because of each pulse has a high power, lead to rise the temperature load on the work piece and the workpiece melt and vaporize faster [26], [27]. High duty cycle leads to conducting the discharge for long period lead to rise in MRR, [28] and the Slight increase of MRR is due to some reasons like flushing effect of dielectric.

Figure 8 is the surface curve fitting plot present the effect of spark duration time and material on MER. It is clarified that Material erosion rate decreases as the pulse duration increase, which lead to increase the percent of reinforcement particles that became free in the composite. Because of the shielding and protecting effect of reinforcement particles Al_2O_3 in the composites and Al_2O_3 being insulated material will decrease both the electrical and thermal conductivity, so the spark energy transferred to the material also decreases. Reinforcement particles are retarding the penetration of the spark into the material. Hence an increase in the volume fraction of the composite material reduces the material erosion rate[29],[30].

B. Effect of process parameters on EWR

In Fig. 9, main effect plots for S/N signal to noise ratio of electrode wear rate (EWR) for graphite electrode is plotted. It is very clear from the main effect plots that current (A) is the most significant process parameter, while materials (D), pulse duration time (B) and duty cycle (C) possess the following effect respectively.From Fig. 9, According to the lower-the-better quality criteria for EWR of graphite electrode, based on the minimum point on the graph, the optimum condition for each factor indicated is A3 (5 A), B1(50 µs), C3 (87 %), D2 (0.5 v%). The mean S/N ratio table for electrode wear rate is Table 11. When using graphite electrodes, the impact of process parameters can be ranked as follows (current, material, pulse duration time and duty cycle).

Table 12 shows the ANOVA results for electrode wear rate. The ANOVA table presents the contribution percentage and the statistical

significance of each parameter. Therefore, comparing between the P-value and generally used α-level = 0.05, it is found that if the P-value for each parameter is less than or equal to α, it can be indicated that the impact of this parameter is significant, otherwise it is not significant impact. The most effective parameter on EWR is pulse duration time (B) with contribution percentage (48.29%) followed by current (a) 24.56%, material (D) 18.83% and duty cycle (C) 3.10% is the least effective parameter.

The mathematical model is developed to relate the response parameters EWR with their machining parameters (current, spark duration time, material and duty cycle).

$$\mathbf{EWR} = -5.277673456 + 2.421183417\text{x}10^{-1}\,\text{A} - 2.968080323\text{x}10^{-3}\,\text{B} + 1.170204193\text{x}10^{-1}\,\text{C} - 2.058171721\text{x}10^{-1}\,\text{D} + 1.6379273\text{x}10^{-4}\,\text{AB} - 2.741136698\text{x}10^{-3}\text{A C} - 1.27107125\text{x}10^{-2}\text{AD} + 1.738162738\text{x}10^{-5}\,\text{BC} + 1.767703402\text{x}10^{-5}\text{B D} + 2.45867088\text{x}10^{-3}\,\text{C D} - 1.218867675\text{x}10^{-3}\text{A}^2 + 2.532109912\text{x}10^{-6}\,\text{B}^2 - 6.408539555\text{x}10^{-4}\text{C}^2 + 4.012798512\text{x}10^{-2}\text{D}^2 \quad \ldots$$

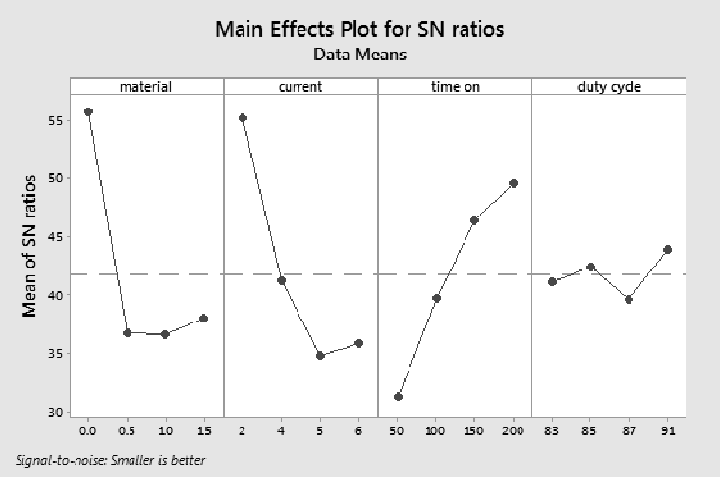

Fig. 9 Main effects plot for S/N ratios of each factor on EWR.

Table 10S/N ratio response table for EWR

Level	Material	Current	Time on	Duty cycle
1	55.77	55.18	31.28	41.09
2	36.7	41.28	39.77	42.37
3	36.59	34.74	46.41	39.65
4	37.98	35.85	49.59	43.94
Delta	19.18	20.44	18.32	4.29
Rank	2	1	3	4

Table 11 ANOVA results for EWR.

Sequence of variation	Degrees of freedom (DF)	Sum of squares (SS)	Mean square MS = SS/DF	Contribution	P-Value
material	3	0.003183	0.001061	18.83%	0.16
current	3	0.004152	0.001384	24.56%	0.118
time on	3	0.008166	0.002722	48.29%	0.05
duty cycle	3	0.000525	0.000175	3.10%	0.66
Error	3	0.000882	0.000294	5.22%	
Total	15				

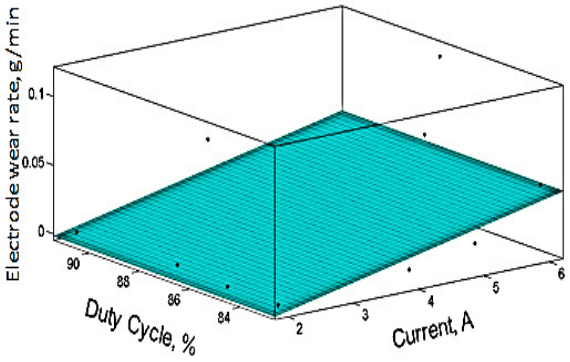

Fig. 10: Surface plot of electrode wear rate versus current and duty cycle.

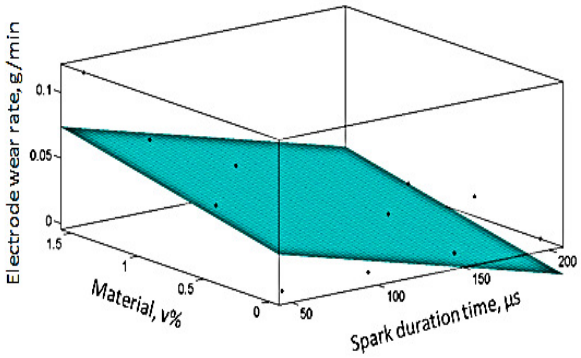

Fig. 11: Surface plot of electrode wear rate versus material and spark duration time.

The surface curve fitting plot of first polynomial degree present the relative effect of current and duty cycle on EWR as it is presented in Fig. 10. It is clarified that the EWR Increases significantly with increasing the current and this increase becomes more with increasing the duty cycle. It was demonstrated, high current increase the arc energy and thus higher heat flux leads to increase the melt and evaporation of the electrode.it be can noticed clearly, the direct impact of the current on TWR. [31]

Figure 11 is the surface curve fitting plot present the effect of spark duration time and material on EWR. It is clarified that the EWR Increases significantly with decreasing the spark duration time and increase with increasing the reinforcement particles. A longer duration of pulse increases EWR during the initial period and thereafter it decreases due to formation of craters and the resistance of the conductive channel due to the removed reinforcement particles. [30]

***C.* Effect of process parameters on SR**

In Fig. 12,main effect plots for S/N signal to noise ratio of surface roughness (SR) is plotted. As it clarified It is very clear from the main effect plots that current (A) is the most significant process parameter, while pulse duration time (B), material (D) and duty cycle (C) possess the following effect respectively.From Fig. 12, according to the lower-the-better quality criteria for SR, based on the minimum point on the graph, the optimum condition for each factor indicated is A4 (6 A), B4 (200 µs), C4 (91%), D3 (1 v%).

The mean S/N ratio table for surface roughness is Table 12. The impact of process parameters can be ranked as follows (current, pulse duration time, material and duty cycle).

Tables 13 shows the ANOVA results for electrode wear rate. The ANOVA table presents the contribution percentage and the statistical significance of each parameter. Therefore, comparing between the P-value and generally used α-level = 0.05, it is found that if the P-value for each parameter is less than or equal to α, it can be indicated that the impact of this parameter is significant, otherwise it is not significant impact. The most effective parameter on SR is current (A) with contribution percentage (86.52%) followed by spark duration time (B) 3.79%, material (D) 1.64% and duty cycle (C) 1.35% is the least effective parameter. The mathematical model is developed to relate the response parameters SR with their machining parameters (current, spark duration time, material and duty cycle).

The surface plot of a first polynomial degree present the relative effect of current and duty cycle on SR as it is shown in Fig. 13. It is clarified that the discharge current has a more pronounced effect while the duty cycle doesn't have a crucial influence on the SR as the discharge current increases, the heat load concentration increases on the machined surface, which results in discontinuous spots of recast surface, cracks on recast layer, deeper craters and non- homogeneous distribution of craters on machined surface [32-33]. High duty factor means

higher plasma channel energy, which tend to increase the SR [28]

Figure 14 the surface plot was presented the effect of spark duration time and material on SR, It is clarified That SR increases significantly with increasing the spark on time and the material volume friction. Although spark duration time does not have a significant effect, however, at the low spark duration time SR increases due to high concentration of the spark energy forming a deep crater, but SR decreases with increase the spark time due to the expansion of the plasma channel in the discharge gap producing a wide shallow crater [34]. At very high spark temperature, bond between reinforcement and base metal breaks. Due to this reinforcement embedded in base metal become free and craters are created at the place. As a result of the increasing of reinforcement particles, the number of craters on unit area also increases. And thus the SR increases. [29]

SR

$$= 936.1351763 - 22.07353942\,A + 1.769007706x10^{-1}\,B - 20.77574305\,C + 25.75097538\,D - 2.121774325x10^{-2}\,AB + 2.634433276x10^{-1}\,AC + 8.380647097x10^{-1}\,AD + 4.053849982x10^{-5}BC - 1.690785793x10^{-2}BD - 2.692658099x10^{-1}\,CD + 2.628695737x10^{-1}\,A^2 - 2.580840771x10^{-4}\,B^2 + 1.138403675x10^{-1}\,C^2 - 3.814372373\,D^2 \ldots\ldots\ldots\ldots ($$

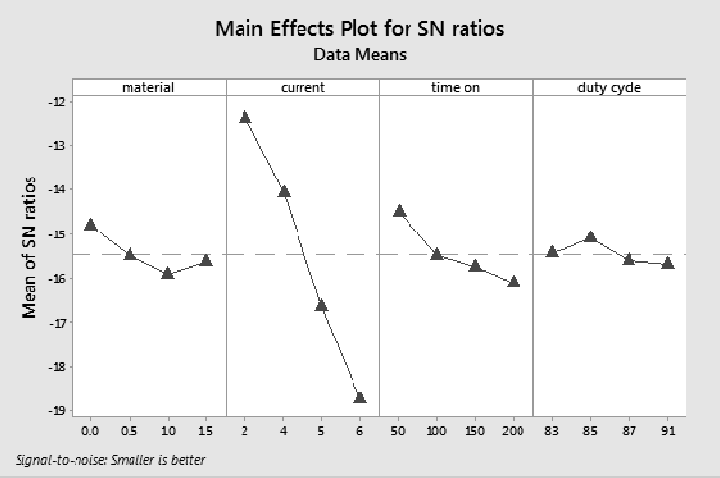

Fig. 12 Main effects plot for S/N ratios of each factor on SR.

Table 12 S/N ratio response table for SR

Level	Material	Current	Time on	Duty cycle
1	-14.8	-12.37	-14.51	-15.45
2	-15.48	-14.07	-15.48	-15.1
3	-15.92	-16.64	-15.73	-15.6
4	-15.62	-18.76	-16.12	-15.69
Delta	1.12	6.39	1.61	0.59
Rank	3	1	2	4

Table 13 ANOVA results for SR

Sequence of variation	Degrees of freedom (DF)	Sum of squares (SS)	Mean square MS = SS/DF	Contribution	P-Value
material	3	0.744	0.248	1.35%	0.89
current	3	47.8045	15.9348	86.52%	0.032
time on	3	2.0965	0.6988	3.79%	0.674
duty cycle	3	0.9088	0.3029	1.64%	0.86
Error	3	3.6957	1.2319	6.69%	
Total	15				

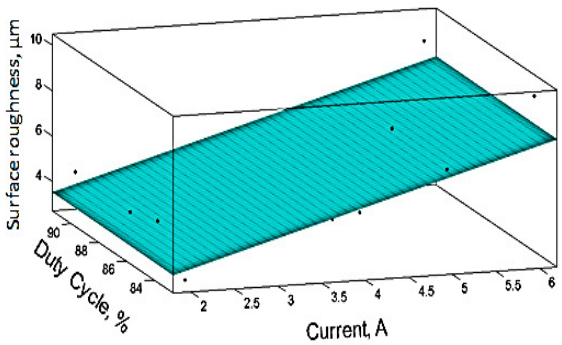

Fig. 13: Surface plot of surface roughness versus current and duty cycle.

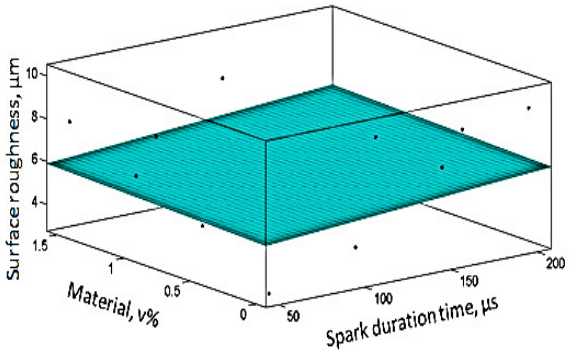

Fig. 14: Surface plot of surface roughness versus material and spark duration time.

D. **Effect of process parameters on 2GS**

In Fig. 15, main effect plots for S/N signal to noise ratio of gap side (2GS) is plotted as it is presented. It is very clear from the main effect plots that current (A) is the most significant process parameter, while material (C), pulse duration time (B) and duty cycle (C) possess the following effect respectively. From Figure 15, According to the lower-the-better quality criteria for 2GS, based on the minimum point on the graph, the optimum condition for each factor indicated is A4 (6 A), B4 (200 µs), C3 (87 %), D4 (1.5 v%).

The mean S/N ratio table for gap side Table 14. The impact of process parameters can be ranked as follows (current, material, pulse duration time and duty cycle).

Tables 15 shows the ANOVA results for electrode wear rate. The ANOVA table presents the contribution percentage and the statistical significance of each parameter. Therefore, comparing between the P-value and generally used α-level = 0.05, it is found that if the P-value for each parameter is less than or equal to α, it can be indicated that the impact of this parameter is significant, otherwise it is not significant impact. The most effective parameter on 2GS is current (A) with contribution percentage (70.57%) followed by material (D) 21.04%, spark duration time (B) 1.81% and duty cycle (c) 2.54% is the least effective parameter.

The mathematical modelis developed to relate the response parameters (2GS) with their machining parameters (current, spark duration time, material and duty cycle).

The surface curve fitting plot of a first polynomial degree presents the relative effect of current and duty cycle on 2GS as it is shown Fig. 16. It is clarified that is the 2GS Increases significantly with increasing the current while the duty cycle has not a pronounced effect it may be due to the combined effect of high current and injection flushing where the second discharge happen during the ejection of debris. Due to high the current, the second discharge or spark jumping are performed at high energy leading to increase 2GS

Figure 17 1is the surface curve fitting plot present the effect of spark duration time and material on 2GS.It is clarified that the 2GS Increases slightly with increasing the reinforcement particles and almost there is no effect of spark duration time on gap side. It can be due to the erosion effect of ceramic particles after the side discharge

$$\mathbf{2GS} = 22.15344393 - 5.652192808x10^{-1}A + 9.781369634x10^{-3}\,B - 3.197343927x10^{-2}C + 0.397667648\,D - 1.047106789x10^{-4}\,A\,B + 6.918693049x10^{-3}\,AC - 7.25921875x10^{-3}AD - 9.445963294x10^{-5}\,BC - 5.527621611x10^{-4}\,BD - 3.913433718x10^{-3}CD + 2.26107353x10^{-3}\,A^2 - 2.917864506x10^{-6}\,B^2 + 1.054935656x10^{-4}\,C^2 + 4.056027136x10^{-2}D^2 \ldots\ldots\ldots\ldots (15)$$

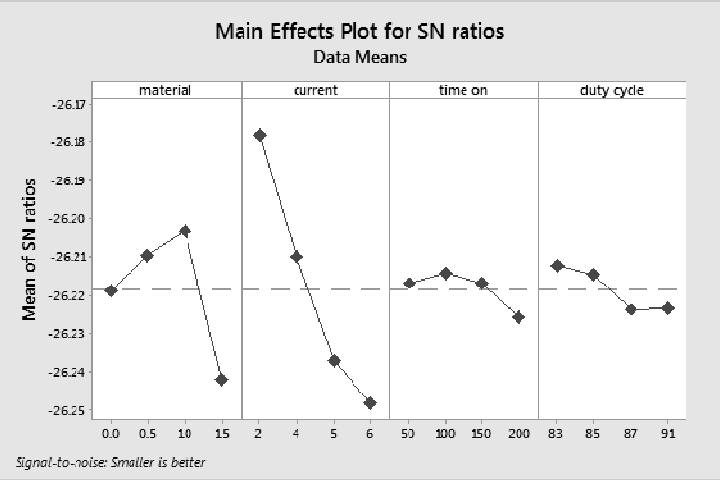

Fig. 15 Main effects plot for S/N ratios of each factor on 2GS.

Table 14 S/N ratio response table for 2GS

Level	Material	Current	Time on	Duty cycle
1	-26.22	-26.18	-26.22	-26.21
2	-26.21	-26.21	-26.21	-26.21
3	-26.2	-26.24	-26.22	-26.22
4	-26.24	-26.25	-26.23	-26.22
Delta	0.04	0.07	0.01	0.01
Rank	2	1	3	4

Table 15 ANOVA results for 2GS

Sequence of variation	Degrees of freedom (DF)	Sum of squares (SS)	Mean square MS = SS/DF	Contribution	P-Value
material	3	0.019259	0.00642	21.04%	0.105
current	3	0.06461	0.021537	70.57%	0.021
time on	3	0.001654	0.000551	1.81%	0.738
duty cycle	3	0.002326	0.000775	2.54%	0.644
Error	3	0.003707	0.001236	4.05%	
Total	15				

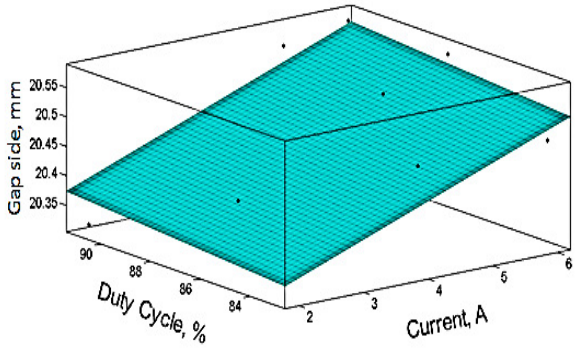

Fig. 16: Surface plot of gap side versus current and duty cycle.

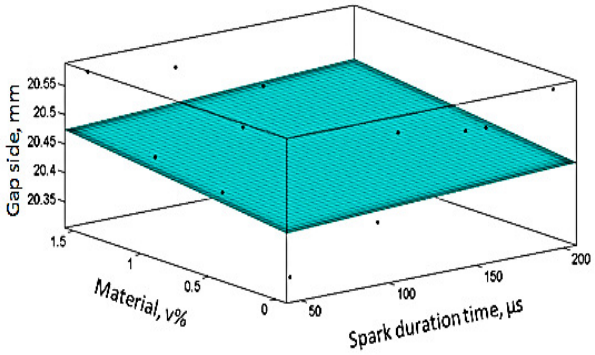

Fig. 17: Surface plot of gap side versus material and spark duration time.

VI. CONCLUSION

This investigation studies the effect of EDM parameters on the machining of Al 6063/Al2O3 metal matrix composite using graphite electrode based on Taguchi approach. Leading to the following conclusions:

(1) Among the four specified EDM parameters, current (I) possess the most significant impact on material erosion rate, electrode wear rate, surface roughness and gap side.

(2) Material erosion rate, electrode wear rate, surface roughness and gap side are not a crucial affected with duty cycle.

(3) The most effective parameter on MER is current (95.98%) followed by spark duration time (2.06%), duty cycle (1.10%) and material (0.071%) is the least effective parameter with graphite electrode. Maximum MRR was verified from high current, low spark duration time, high duty cycle and zero concentration of reinforcement particles.

(4) The most effective parameter on EWR is pulse duration time (48.29%) followed by current (24.56%), material (18.83%) and duty cycle (3.10%). Minimum SR was obtained at high current, high spark duration time, high duty cycle and 1% concentration of reinforcement particles.

(5) The most effective parameter on SR is current (86.52%) followed by spark duration time (3.79%), material (1.64%) and duty cycle(1.35%). Minimum EWR was verified from high current, low spark duration time, high duty cycle and 0.5% concentration of reinforcement particles.

(6) The most effective parameter on 2GS is current (70.57%) followed by material (21.04%), spark duration time (1.81%) and duty cycle (2.54%). Minimum 2GS was verified from high current, high spark duration time, high duty cycle and 1.5% concentration of reinforcement particles.

VII. REFERENCES

[1] S. A. Sajjadi, H. R. Ezatpour, and M. T. Parizi, "Comparison of microstructure and mechanical properties of A356 aluminum alloy/Al2O3 composites fabricated by stir and compo-casting processes," Mater. Des., vol. 34, pp. 106–111, 2012.

[2] K. K. Alaneme and M. O. Bodunrin, "Corrosion behavior of alumina reinforced aluminium (6063) metal matrix composites," J. Miner. Mater. Charact. Eng., vol. 10, no. 12, p. 1153, 2011.

[3] P. N. Singh, K. Raghukandan, M. Rathinasabapathi, and B. C. Pai, "Electric discharge machining of Al--10% SiCP as-cast metal matrix composites," J. Mater. Process. Technol., vol. 155, pp. 1653–1657, 2004.

[4] P. Srikanth and C. P. Kumar, "Electrical Discharge Machining Characteristics of Aluminium Metal Matrix Composites-A

Review," Int. J. Sci. Res., vol. 4, pp. 1–15, 2013.
[5] M.-D. Moses and M. P. Jahan, "Micro-EDM machinability of difficult-to-cut Ti-6Al-4V against soft brass," Int. J. Adv. Manuf. Technol., vol. 81, no. 5–8, pp. 1345–1361, 2015.
[6] B. M. Schumacher, "After 60 years of EDM the discharge process remains still disputed," J. Mater. Process. Technol., vol. 149, no. 1–3, pp. 376–381, 2004.
[7] R. L. Boxman, D. M. Sanders, and P. J. Martin, Handbook of vacuum arc science & technology: fundamentals and applications. William Andrew, 1996.
[8] A. Descoeudres, "Characterization of electrical discharge machining plasmas," 2006.
[9] K. Hemalatha, V. S. K. Venkatachalapathy, and N. Alagumurthy, "Processing and synthesis of metal matrix Al 6063/Al_2O_3 Metal Matrix Composite by stir casting process," Int. J. Eng. Res. Appl., vol. 3, no. 6, pp. 1390–1394, 2013.
[10] H. C. Lee and M. S. Kim, "A Fabrication Method of Aluminium Short Fibre Aluminia Matrix Composites by Compocasting," in Proceedings of the KSME-JSME Joint Conference, 1990, pp. 471–475.
[11] J. J. Rino, D. Sivalingappa, H. Koti, and V. D. Jebin, "Properties of Al6063 MMC reinforced with zircon sand and alumina," IOSR J. Mech. Civ. Eng., vol. 5, no. 5, pp. 72–77, 2013.
[12] S. K. Dewangan and A. Arora, "Mechanical Properties of Aluminum 6063 Alloy based Graphite Particles Reinforced Metal Matrix Composite," IJSRD-International J. Sci. Res. Dev., vol. 3, no. 05, pp. 613–2321, 2015.
[13] K. C. Russell, J. A. Cornie, and S. Y. Oh, "Interfaces in metal-matrix composites," in Proceedings of a TMS Symposium, AK Dhingra and SG Fishman, eds., The Metallurgical Society, 1986, p. 61.
[14] W. Zhou and Z. M. Xu, "Casting of SiC reinforced metal matrix composites," J. Mater. Process. Technol., vol. 63, no. 1–3, pp. 358–363, 1997.
[15] C. A. Reddy and E. Zitoun, "Tensile behavior of 6063/Al^ sub 2^ o^ sub 3^ particulate metal matrix composites fabricated by investment casting process," Int. J. Appl. Eng. Res., vol. 1, no. 3, p. 542, 2010.
[16] A. Mortensen, J. A. Cornie, and M. C. Flemings, "Solidification processing of metal-matrix composites," JOM, vol. 40, no. 2, pp. 12–19, 1988.
[17] M. K. Aravindan, K. Balamurugan, and G. Murali, "Effect of reinforcement of AL-6063 with SiC on mechanical behavior and microstructure of metal matrix composites," Carbon Sci. Technol., vol. 6, no. 2, pp. 388–394, 2014.
[18] L. Salvo, G. L'esperance, M. Suery, and J. G. Legoux, "Interfacial reactions and age hardening in Al? Mg? Si metal matrix composites reinforced with SiC particles," Mater. Sci. Eng. A, vol. 177, no. 1–2, pp. 173–183, 1994.
[19] K. MIWA and T. OHASHI, "Preparation of fine SiC particle reinforced Al alloy composites by compocasting process," Achiev. Compos. Japan United States, pp. 355–362, 1990.
[20] M. K. Surappa and P. K. Rohatgi, "Technical note," Met. Technol., vol. 5, no. 1, pp. 358–361, 1978.
[21] J. W. McCoy, C. Jones, and F. E. Wawner, "Preparation and properties of cast ceramic aluminum composites," SAMPE QUARTERLY-SOCIETY Adv. Mater. Process Eng., vol. 19, no. 2, pp. 37–50, 1988.
[22] W. M. Zhong, G. Lesperance, and M. Suery, "Interfacial reactions in Al-Mg (5083)/SiCp composites during fabrication and remelting," Metall. Mater. Trans. A, vol. 26, no. 10, pp. 2637–2649, 1995.
[23] W. Wang and F. Ajersch, "Particle Interaction of Melt-Stirred Al--Si/SiC sub p Composites," Adv. Prod. Fabr. Light Met. Met. Matrix Compos., pp. 629–641, 1992.
[24] W. Wang, F. Ajersch, and J. P. A. Löfvander, "Si phase nucleation on SiC particulate reinforcement in hypereutectic Al? Si alloy matrix," Mater. Sci. Eng. A, vol. 187, no. 1,

pp. 65–75, 1994.
[25] P. K. Rohatgi, R. Asthana, and S. Das, “Solidification, structures, and properties of cast metal-ceramic particle composites,” Int. Met. Rev., vol. 31, no. 1, pp. 115–139, 1986.
[26] H. A. Hegab, M. H. Gadallah, and A. K. Esawi, “Modeling and optimization of Electrical Discharge Machining (EDM) using statistical design,” Manuf. Rev., vol. 2, p. 21, 2015.
[27] A. Equbal, A. K. Sood, M. A. Equbal, and M. I. Equbal, “An Investigation on Material Removal Rate of EDM Process: A Response Surface Methodology Approach,” World Acad. Sci. Eng. Technol. Int. J. Mech. Aerospace, Ind. Mechatron. Manuf. Eng., vol. 11, no. 4, pp. 856–861, 2017.
[28] S. H. Aghdeab and N. G. Ghazy, “Effect of Current and Duty Factor for Different Electrode Shapes on Material Removal Rate in EDM,” Eng. Technol. J., vol. 36, no. 6 Part (A) Engineering, pp. 633–640, 2018.
[29] R. N. Marigoudar and K. Sadashivappa, “Effect of machining parameters on MRR and surface roughness in machining of ZA43/SiCp composite by WEDM,” Int. J. Appl. Sci. Eng., vol. 11, no. 3, pp. 317–330, 2013.
[30] V. Senthilkumar and B. U. Omprakash, “Effect of Titanium Carbide particle addition in the aluminium composite on EDM process parameters,” J. Manuf. Process., vol. 13, no. 1, pp. 60–66, 2011.
[31] V. Krishnaraj, “Optimization of Process Parameters in Micro-EDM of Ti-6Al-4V Alloy,” J. Manuf. Sci. Prod., vol. 16, no. 1, pp. 41–49, 2016.
[32] A. T. Salcedo, I. P. Arbizu, and C. J. L. Pérez, “Analytical modelling of energy density and optimization of the EDM machining parameters of Inconel 600,” Metals (Basel)., vol. 7, no. 5, p. 166, 2017.
[33] S. Gopalakannan, T. Senthilvelan, and K. Kalaichelvan, “Electrical discharge machining of hybrid metal matrix composites by applying Taguchi method,” Int. J. Manuf. Technol. Manag., vol. 26, no. 1–4, pp. 114–136, 2012.
[34] M. K. Das, K. Kumar, T. K. Barman, and P. Sahoo, “Prediction of surface roughness in edm using response surface methodology and artificial neural network,” J. Manuf. Technol. Res., vol. 6, no. 3/4, p. 93, 2014.
[35] F. L. Amorim and W. L. Weingaertner, “The behavior of graphite and copper electrodes on the finish die-sinking electrical discharge machining (EDM) of AISI P20 tool steel,” J. Brazilian Soc. Mech. Sci. Eng., vol. 29, no. 4, pp. 366–371, 2007.